

Diagnosing Breast Cancer with the Aid of Fuzzy Logic Based on Data Mining of a Genetic Algorithm in Infrared Images

Hossein Ghayoumi Zadeh*, Omid Pakdelazar**, Javad Haddadnia*[♦],
Gholamali Rezai-Rad**, Mohammad Mohammad-Zadeh***

*Biomedical Engineering Department, Hakim Sabzevari University, Sabzevar, Khorasan Razavi, Iran

**Department of Electrical and Electronic Engineering, Iran University of Science and Technology, Tehran, Iran

***Department Of Physiology and Pharmacology, School of Medicine, Sabzevar University of Medical Sciences, Sabzevar, Khorasan Razavi, Iran

Abstract

Background: Breast cancer is one of the most prevalent cancers among women today. The importance of breast cancer screening, its role in the timely identification of patients, and the reduction in treatment expenses are considered to be among the highest sanitary priorities of a modern country. Thermal imaging clearly possesses a special role in this stage due to rapid diagnosis and use of harmless rays.

Methods: We used a thermal camera for imaging of the patients. Important parameters were derived from the images for their posterior analysis with the aid of a genetic algorithm. The principal components that were entered in a fuzzy neural network for clustering breast cancer were identified.

Results: The number of images considered for the test included a database of 200 patients out of whom 15 were diagnosed with breast cancer via mammography. Results of the base method show a sensitivity of 93%. The selection of parameters in the combination module gave rise measured errors, which in training of the fuzzy-neural network were of the order of clustering 1.0923×10^{-5} , which reached 2%.

Conclusion: The study indicates that thermal image scanning coupled with the presented method based on artificial intelligence can possess a special status in screening women for breast cancer due to the use of harmless non-radiation rays. There are cases where physicians cannot decisively say that the observed pattern in the image is benign or malignant. In such cases, the response of the computer model can be a valuable support tool for the physician enabling an accurate diagnosis based on the type of imaging pattern as a response from the computer model.

Keywords: Adaptive Neuro Fuzzy Inference System (ANFIS), Breast cancer, Thermograph, Genetic algorithm, artificial neural net

[♦]Corresponding Author:

Javad Haddadnia, Associate Professor of Biomedical Engineering, Biomedical Engineering Department, Hakim Sabzevari University, Sabzevar, Khorasan Razavi, Iran.
Email: haddadnia@hsu.ac.ir

Introduction

Breast cancer usually appears in the ducts that transport milk to the nipple and the lobules of glands that produce milk. Cancer is a disease rooted in a social, cultural and economic structure as well as social behavior, political agendas, individual behavior and function of cells and their items.^{1,2} Breast cancer is one of the most widespread cancers. According to figures from the America National Cancer Institute, one woman in eight will be afflicted with breast cancer in her life.³ Breast cancer recognized at an early stage can usually be treated. The Gynecologist emphasizes to the patient suspicious of breast cancer to seek medical attention in the initial stages of the illness. In this way the treatment outcome will usually be more favorable for the patient and the healthcare service.⁴ It is significant to note that due to improved detection methods, the number of cancer patients has increased; nevertheless the mortality rate has fallen. Studies show that early detection can lead to an 85% chance for survival compared to 10% for late detection.⁵ Breast cancer is the most commonly diagnosed cancer in females accounting for about 30% of cancers.⁶ It also occurs in males; however, the frequency is significantly lower in the latter group. During 2003–2007, the average mortal age for breast cancer was 68 years. The approximate percentages of deaths due to breast cancer according to age group is as follows: under 20(0.0%), 20-34 (0.9%), 35-44 (6.0%), 45-54 (15.0%), 55-64 (20.8%), 65-74 (19.7%), 75-84 (22.6%) and above 85 (15.1%) years.⁷ It has been reported that diagnosis according to age group was 0% for under 20 years of age, 1.9% (20-34), 10.2% (35-44), 22.6% (45-54), 24.4% (55-64), 19.7% (65-74), 15.5% (75-84), and 5.6% for those above the age of 85 years.⁷

Early detection is the key factor for successful breast cancer treatment. Some diagnostic techniques such as clinical examination, ultrasound, mammography, magnetic resonance and thermography⁸⁻¹¹ are employed to detect and provide an accurate diagnosis of breast cancer.

Mammography is considered the most favored

test;¹² nevertheless, it is not effective for fibrocystic diagnosis in dense or surgically implanted breasts. Dense breasts are common in women around 40 years of age. Mammographic examination presents the risk of ionizing radiation and the discomfort of compression. In the search for other techniques, thermography has emerged as a potential method to complement mammography and improve the efficiency of overall detection.^{13,14} Thermography is a non-invasive, economic, rapid diagnostic method that does not touch the patient and does not inflict pain.^{12,13,15} Additionally it is risk-free and does not emit ionizing radiation.^{14,16} This method is simple and is based on quantification of the surface temperature of the body measuring infrared radiation emitted by human skin.^{12,13}

In 1982, the US Food and Drug Administration (FDA) approved InfraRed Thermography (IRT) as an adjunct tool for the diagnosis of breast cancer. Kennedy et al., in a recent review, presented a comparative study of IRT and other imaging techniques for breast screening and have concluded that IRT provides additional functional information on the thermal and vascular condition of the tissues.¹⁷

Ng presented an excellent review of IRT as a non-invasive breast tumor detection modality, where he described in detail the basic methodology, standard practices, image capture and image analysis.¹⁸ According to Ng, an abnormal breast thermogram was indicative of significant biological risk. Tumors generally have an increased blood supply and an increased metabolic rate which leads to localized high temperature spots over those areas, rendering them relatively easy to detect by IRT. Apart from passive breast imaging, cold stimulation-based imaging procedures are also in practice.¹⁹ Blood vessels produced by cancerous tumors are simple endothelial tubes devoid of a muscular layer. Such blood vessels fail to constrict in response to sympathetic stimulus like a sudden cold stress and show a hyperthermic pattern due to vasodilatation. Deng and Liu have shown that induced evaporation enhances thermographic

contrast in cases of tumors that are underneath the skin.²⁰

This study focused on the creation of an information bank for thermal imaging or thermography. The clustering of the samples in thermal images was undertaken based on fuzzy-neural logic. Some difficulties were encountered due to the sheer volume of the samples. The neural-fuzzy module could not cluster all of the samples, taking into consideration the full scope of the parameters. To remedy this, a combination module was designed from a genetic algorithm and artificial net in order to decrease the diagnostic parameters.

Although, the use of thermal cameras dates back to the 1960s, new research began in the late 1990s. The initial work was centered on the identification of cancer by imaging. Physicians diagnosed cancer by thermal imaging, after which the illness was classified via further image analysis.²¹ It should be pointed out that this method was not suitable for the population in general as it presented a rather laborious task. The sheer volume of images limited the possibility of efficient revision and diagnosis. An alternative method was asymmetric thermal imaging; however, the low associated image quality limited its success.²² Intelligent identification by software based on detachment of all of the unique parts (thermal red parts) of the image showed the extracted parts, however it required revision by a physician. The system could not specifically extract tumor images, but just extracted the thermal part.²³

Keyserlingk and associates published a retrospective study that reviewed the relative ability of clinical examinations, mammography, and infrared imaging in an attempt to detect 100 new cases of ductal carcinoma in situ, stage I and 2 breast cancers. Results from the study found that the sensitivity for clinical examination alone was 61%, mammography alone was 66%, and infrared imaging alone was 83%. When suspicious and equivocal mammograms were combined, the sensitivity was increased to 85%. A sensitivity of 95% was found when suspicious, equivocal

mammograms were combined with abnormal infrared images. However, when clinical examination, mammography, and infrared images were combined a sensitivity of 98% was reached.²⁴

In this paper,²⁵ it is shown that Complementary Learning Fuzzy Neural Network (CLFNN) complements breast thermography in various ways. The combination of breast thermography and CLFNN gives rise to more consistent results than merely using breast thermography. Whether it is cancer detection, tumor classification or breast cancer diagnosis (multi-class problem), CLFNN outperforms conventional methods, showing the strength of complementary learning in the recognition task. FALCON-AART assists physicians in distinct diagnostic tasks by providing a relatively accurate decision support tool, which could potentially enhance patient outcome. FALCONAART not only gives superior results compared with conventional methods, but it also offers intuitive positive and negative fuzzy rules to explain its reasoning process.

Materials and Methods

The necessary information for this study was obtained from research undertaken at Sabzevar University, Sabzevar, Iran, with the cooperation of Sabzevar University of Medical Sciences. The sample population consisted of 200 women aged from 18 to 35 years. The group had 15 unnatural growths in their breasts. Information was collected as follows. Initially, patients underwent thermal imaging, after which the images were processed.

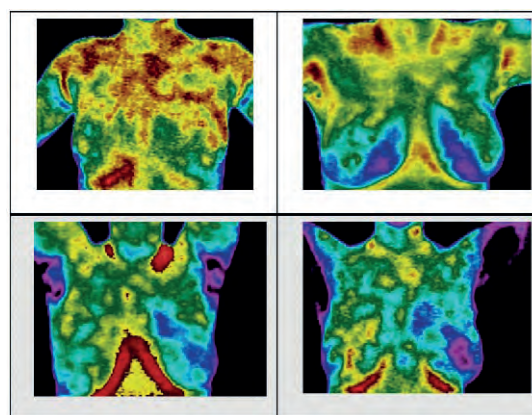


Figure 1. A sample from the existing images in the database which have been imaged by the camera for processing stages of the images.

Subsequently, the extracted results were subjected to a genetic algorithm and neural network stage for data optimization. The extracted properties of thermal images were: 1) patient age, 2) mean, 3) difference between two breast areas, 4) variance, 5) skewness, 6) kurtosis, 7) entropy, and 8) thermal pattern.^{26,27}

Image processing

Samples of the images obtained are shown in Figure 1.

The first step of this method is the diagnosis of the breast area and detachment. For this purpose, we used a gray image. The stages of the image processing on thermal images are shown in the flowchart in Figure 2.

The component of image intensity directly depends on thermal energy delivery to correlated areas. A histogram expresses the delivery intensity. It explains image combination. The moments of the histogram give statistical information about the texture of the image. Four amounts of mean, variance, skewness and kurtosis have been given, expressed as follows:^{28,29}

$$\text{Mean } \mu = \frac{1}{N} \sum_{j=1}^N p_j \quad (1)$$

$$\text{Variance } \sigma^2 = \frac{1}{N-1} \sum_{j=1}^N (p_j - \mu)^2 \quad (2)$$

$$\text{Kurtosis} = \frac{1}{N} \sum_{j=1}^N \left(\frac{p_j - \mu}{\sigma} \right)^4 \quad (3)$$

$$\text{Skewness} = \frac{1}{N} \sum_{j=1}^N \left(\frac{p_j - \mu}{\sigma} \right)^3 \quad (4)$$

$$\text{Entropy } H(X) = \sum_{j=1}^N p_j \log p_j \quad (5)$$

Where p_j is the probability density of the j th bin in the histogram and N is the total number of bins. Skewness is a measure of symmetry, or more precisely, the lack of symmetry. Kurtosis is a measure of whether the data are peaked or flat relative to a normal distribution. That is, data sets with high kurtosis tend to have a distinct peak near the mean, decline rather rapidly, and have heavy tails. We use equation 6 to convert the features extracted from left and right sides of breast into a single feature.

$$\left| \frac{\text{feature value from left segment}}{\text{feature value from right segment}} - 1 \right| \quad (6)$$

Thermal pattern

The following steps should be performed:

1. Specify the detachment of the breast area by Circular Hough.
2. Separate the organ by the Sobel edge vector.
3. Pass the image from the filter equation of the method (equation 7)

$$H(x, y) = \begin{cases} 1 & \text{if } \begin{cases} R_{T(x,y)} > 100 \\ G_{T(x,y)} < 20 \\ B_{T(x,y)} < 20 \end{cases} \\ 0 & \text{else} \end{cases} \quad (7)$$

4. Pass the isolated part from the filter of the initial stage.
5. Calculate the area of the arteries and pass from the filter.
6. If there is no suspended area from stage 4, it is not cancerous. If a suspended area is detected, it should be compared with the artery area. If the detected area is larger than the artery area, it would be considered cancerous; otherwise this area would be benign.
7. The code represents the thermal pattern, it

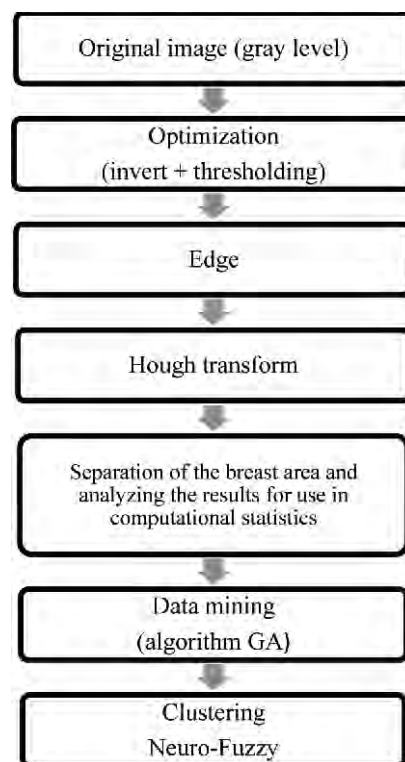


Figure 2. Flowchart and algorithm used for diagnosing asymmetry.

is assigned the value of 1 for the cancerous image in the neural net, otherwise it is 0. To increase convergence in the neural network output, the data input have been normalized for the diagnostic parameters (Table 1).

Data mining

A new generation of techniques and tools are required to assist humans with intelligently analyzing voluminous data and obtain useful conclusions. Knowledge Discovery in Databases (KDD) and Data Mining integrate DataBase Management Systems (DBMS) and artificial intelligence technologies to assist humans in analyzing large quantities of data.

Most data mining algorithms are derived from machine learning, pattern recognition, and statistics. These algorithms include classification, clustering, and graphical models. The primary goals of knowledge discovery are prediction and description. The neural net, as a learning system, is able to describe patterns or tendencies based on historical data and environmental factors while constantly learning in order to improve the results. The most important point is learning or training for the neural net. With training the net adjusts the specific network parameters.

In this research, we employed a three-layer

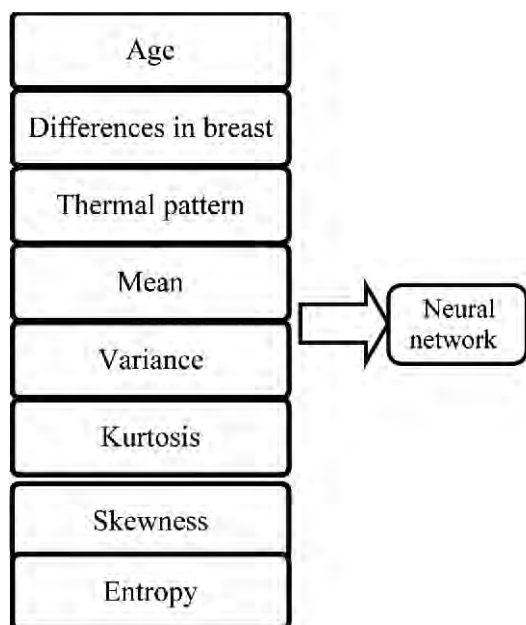


Figure3. The designed neural structure.

Table1. Coding for eight parameters in the neural net.

| | | |
|-----------------------------|-----------|------|
| Age (years) | <20 | F1=1 |
| | 20<age<25 | F1=2 |
| | 25<age<30 | F1=3 |
| | 30<age | F1=4 |
| Differences between breasts | DS<5 | F2=1 |
| | 5<DS<10 | F2=2 |
| | 10<DS<20 | F2=3 |
| | 20<DS | F2=4 |
| Thermal pattern | NO | F3=1 |
| | YES | F3=2 |
| Mean | M<0.5 | F4=1 |
| | 0.5<M<1 | F4=2 |
| | 1<M | F4=3 |
| Variance | M<0.5 | F5=1 |
| | 0.5<M<1 | F5=2 |
| | 1<M | F5=3 |
| Skewness | S<0.5 | F6=1 |
| | 0.5<S<1 | F6=2 |
| | 1<S | F6=3 |
| Kurtosis | K<1 | F7=1 |
| | 1<K<5 | F7=2 |
| | 5<K<10 | F7=3 |
| | 10<K | F7=4 |
| Entropy | E<0.1 | F8=1 |
| | 0.1<E<0.5 | F8=2 |
| | 0.5<E | F8=3 |

Feed-Forward network with a logic activation and leaner function.³⁰ There were eight neurons in the input layer. The middle layer of this network was configured with six neurons. Attention should be paid to the neurons in the middle layer for reducing the time necessary for network training. The mammography result will be the appropriate output of the neural network. The neural network parameterization is shown in Figure 3.

The neural network specification is outlined in Table 2.

The aim of optimization is to determine the group of parameters which would be conditional criterion. In this research, we have used the genetic algorithm and artificial neural network to choose the optimal parameters. Figure 4 shows a block diagram of the system simulated in this study. The Genetic Algorithm (GA) solution is a sequence and hence does not represent a real schedule. The mapping of sequences into schedules during the scheduling process may

cause useful information to be lost. The less similar the operation order is after mapping, the more information would be lost by data mining processes.

First, a binary matrix vector with eight parameters has been accidentally created. The detail of this vector would correspond with the diagnostic parameters in the neural network such that home 1 shows the choice of diagnostic parameters and home 0 corresponds with the genetic algorithm implementation in Table 3.

One criterion is to evaluate the diagnostic screening test insensitivity as a fraction of the number of the appropriately classified patients to the total number of tested patients.^{31,32} In this research the diagnostic sensitivity and specification in the training neural network have been used for calculating the assessment function, which is detailed in equation 8.

$$\text{Fitness} = \frac{TP+TN}{TP+TN+FP+FN} \quad (8)$$

Where, TP is the number of true positive, TN represents the true negative, FP are the false positive and FN, the false negative.

The conditions of stopping the genetic algorithm could be considered the optimal parameter values. The best obtained result has been attained with the combination module detailed in Table 4. If we pay attention to the parameters selected by genetic algorithm, we'll find out that these parameters are correct according to our mental background of thermal images. The chosen parameter B7, which is related to kurtosis, has higher accuracy in calculating statistics related to men or variance. Also the difference between two breast areas is one of the diagnostic methods in asymmetry.

Clustering

In this section, we estimate the ANFIS module.

Table3. The genetic algorithm structure specification.

| | |
|-----|-----------------|
| 80 | Iteration |
| 40 | Population size |
| 0.8 | Crossover |
| 0.1 | Mutation |

Table2. The neural network specifications.

| | |
|------------------|--------------------------------|
| 8 | Number of input layer neurons |
| 1 | Number of hidden layers |
| 1 | Number of output layer neurons |
| 6 | Number of hidden layer neurons |
| Logsig | Activation function |
| Back propagation | Type of network training |
| 0.01 | Mean square error |
| 0.1 | Learning rate |
| 500 | Iteration |

Different structures have been proposed to implement a fuzzy system by neural networks. One of the most powerful of these structures is the structure of the artificial fuzzy neural reasoning system, which is called ANFIS, as developed by Jaris.³³⁻³⁵ The artificial neural fuzzy reasoning system architecture is shown in Figure 5.

The ANFIS, in fact, is a fuzzy reasoning scheme whose system parameters are trained by using NN-based algorithms. Usually determining the linear parameters by using the least square (LSs) algorithm and the membership function (MF) parameters are fine-tuned using a neural network learning method (hybrid learning). Hybrid neuro-fuzzy systems are homogeneous and usually resemble neural networks. The ANFIS main training method is an error propagation method. In this method, the numbers of errors are broadcast using the steepest descending slope algorithm to

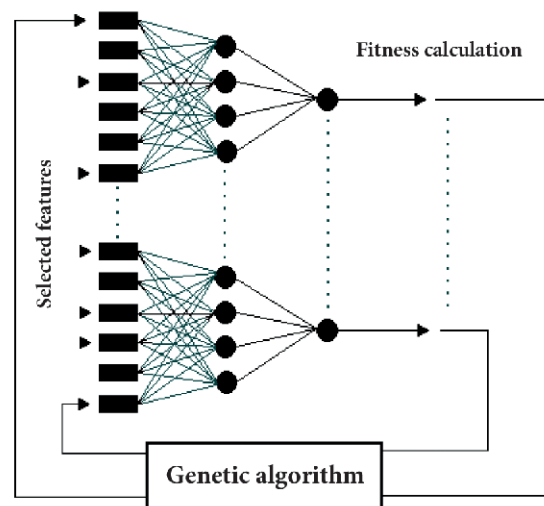


Figure4.Neural network and genetic algorithm combination module.

Table 4. The best obtained result from the chosen parameters in the neural network and the genetic combination module.

| B1 | B2 | B3 | B4 | B5 | B6 | B7 | B8 |
|----|----|----|----|----|----|----|----|
| 0 | 1 | 1 | 0 | 0 | 0 | 1 | 0 |

the inputs and the parameters are corrected. Both neural networks and fuzzy systems have some things in common. They can be used for solving a problem (e.g. pattern recognition, regression or density estimation) if there does not exist any mathematical model of the given problem. They solely do have certain disadvantages and advantages which almost completely disappear by combining both concepts. Neural networks can only come into play if the problem is expressed by a sufficient amount of observed examples. These observations are used to train the black box. On the one hand no prior knowledge about the problem needs to be given. On the other hand, however, it is not straightforward to extract comprehensible rules from the neural network's structure. For simplicity we assume that the fuzzy inference system iii has 2 inputs, x , y , with z as the output. The roll base has two rules as follows:^{36,37}

Rule1: if x is A_1 and y B_1 , then $f_1 = p_1x + q_1y + r_1$ (9)

Rule2: if x is A_2 and y B_2 , then $f_2 = p_2x + q_2y + r_2$

The Sugeno fuzzy model, also known as Takagi–Sugeno–Kang (TSK) model, was proposed to develop a systematic approach to generate fuzzy rules from a given input-output data set (Figure 7). For a two input system, the common fuzzy rule in this model is in the form of:

IF x is A and y is B , THEN $z = f(x, y)$

Where x and y are linguistic variables, A and B are fuzzy sets in the antecedent, and $z = f(x,y)$ is a crisp function in the consequent. Usually, $f(x,y)$ is a polynomial function of the input variables x and y , but it can be any function as long as it can appropriately describe the output of the model within the fuzzy region specified by the antecedent of the rule. When $z = f(x,y)$ is a constant, the system is referred to as a zero-order Sugeno fuzzy model. When $z = f(x,y)$ is a first-order polynomial function, i.e., $px + qy + r$, the resulting FIS is called a first-order Sugeno fuzzy model (Figure 6).

$$Z_1 = p_1x + q_1y + r_1 \quad (10)$$

$$Z_2 = p_2x + q_2y + r_2$$

Weighted average:

$$Z = (w_1z_1 + w_2z_2) / (w_1 + w_2) \quad (11)$$

The ANFIS architectural equivalent is given in Figure 7.

We describe each layer as follows:

LAYER 1. Each node in the first layer employs a node function given by:

$$o_i^1 = \mu_{A_i}(x) \quad (12)$$

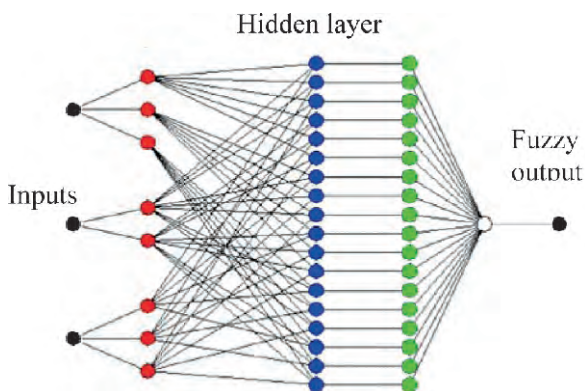


Figure 5. Neural fuzzy network architecture

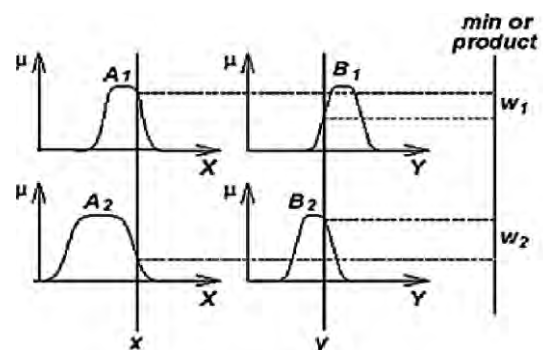


Figure 6. A two-input first-order TSK model.

Where $\mu_{Ai}(x)$ and $\mu_{Bi-2}(y)$ can adopt any fuzzy membership function

LAYER 2. Each node in this layer, labeled Π , calculates the firing Strength of a rule via multiplication:

$$w_i = \mu_{A_i}(x) \times \mu_{B_i}(y), i=1,2. \tag{13}$$

LAYER 3. The i^{th} node in this layer calculates the ratio of the i th rule's firing strength to the sum of all rules' firing strengths:

$$\bar{w}_i = \frac{w_i}{w_1 + w_2}, i=1, 2. \tag{14}$$

LAYER 4. In this layer, each node has the following function:

$$o_i^4 = \bar{w}_i f_i = \bar{w}_i (p_i x + q_i y + r_i) \tag{15}$$

Where w_i is the output of layer 3, and $\{p_i, q_i, r_i\}$ is the parameter set.

LAYER 5. The single node in this layer, labeled Σ , computes the overall output as the sum of all the incoming signals, which is expressed as:

$$o_1^5 = \text{overall output} = \sum_i \bar{w}_i f_i = \frac{\sum_i w_i f_i}{\sum_i w_i}$$

The ANFIS has two sets of adjustable parameters, namely the premise and consequent parameters. During the learning process, the premise parameters in the first layer and the

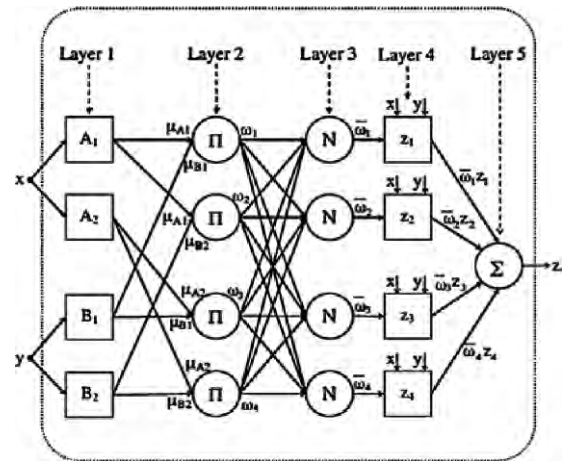


Figure7. ANFIS type 3.

consequent parameters in the fourth layer are tuned until the desired response of the FIS is achieved.³⁸

We create three optimal parameters to enter the neural-fuzzy network by the hybrid model of the genetic algorithm and neural network for training and testing. Samples that are cancerous have an output of 1 whereas healthy samples are assigned an output of 0 in this model. In ANFIS training data from 50% and for checking, 20% of data and test results from 30% of the data were used. Output of the inputs network could be divided into two classes, non-cancerous and cancerous. The graph shows the error to be created during network training in Figure 8. As a consideration, the created error, in repetition 100(epoch), has reached 1.0923×10^{-5} .

The design fuzzy-neural networks surface can be

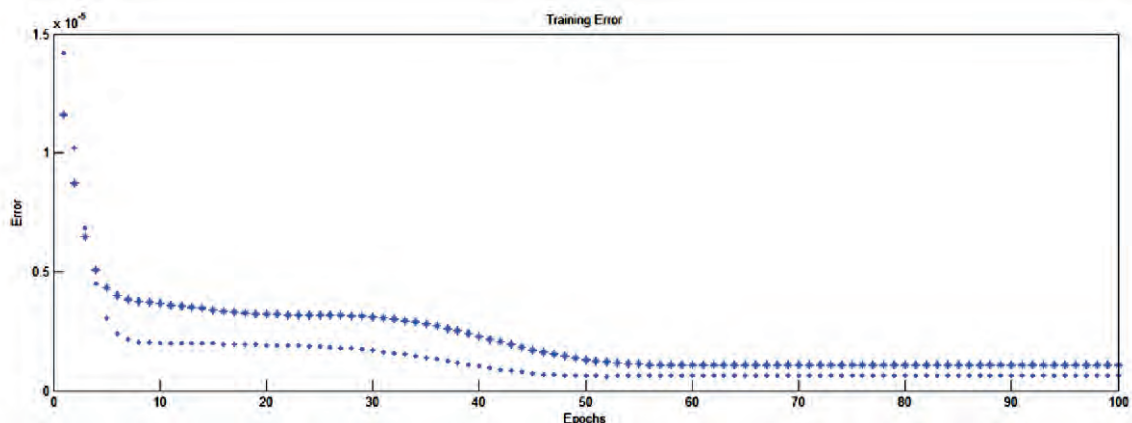


Figure 8. Squared created error in the process of training repetition.

seen in Figure 9.

To evaluate the model, two established bases that included 200 samples were used. The criteria for evaluation of the model were the amount of accuracy, sensitivity, and diagnostic quality together with the bottom level of the ROC curve as the base. Results of the evaluation are seen in Table 5.

In medical diagnostics, test sensitivity is the ability of a test to correctly identify those with the disease (true positive rate), whereas test specificity is the ability of the test to correctly identify those without the disease (true negative rate).

Since sensitivity, accuracy and quality depend to a great extent on the population of dominant patients, we may not be able to compare the efficiency of the network and mammography appropriately and precisely. Thus, the ROC curve analysis was applied to evaluate the efficiency of the model in comparison with mammography results. ROC analysis is a form of measurement mainly used for comparing the efficiency of diagnostic methods. In ROC analysis, the efficiency of the diagnosis is based on two indices: true positive fraction (TPF) and false positive fraction (FPF). The former is a fraction of true malignant cases that were accurately diagnosed (i.e., sensitivity) and the latter is the fraction of benign cases falsely diagnosed as malignant. The ROC curve can be seen in Figure 10.

Regarding the significant results from the sensitivity and ROC curve, the method can be an appropriate pattern in diagnosing and clustering cancer.

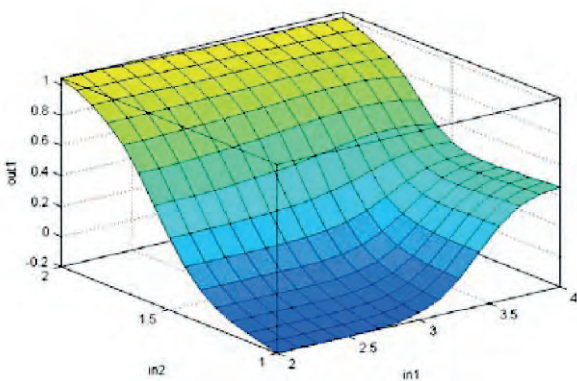


Figure 9. The designed fuzzy-neural network surface.

Table 5. Results from sensitivity and quality in the data base of thermal images.

| | |
|-----|----------------|
| 181 | True negative |
| 14 | True positive |
| 4 | False negative |
| 1 | False positive |
| 93% | Sensitivity |
| 97% | Specificity |

Discussion

Early detection of breast cancer is one of the most important issues that researchers have searched for. If this illness is diagnosed in time, it would be a significant leap forward for reducing the effects and health of the society. Breast cancer is one of the most prevalent contemporary cancers. If it is diagnosed at an early stage, treatment can be much less aggressive and more effective. The results of this research convey that the combination module is able to extract optimal and effective parameters from the diagnostic parameters, thereby facilitating an accurate diagnosis by the physician. In the past, investigation has shown that different intelligent methods have been undertaken to attain a mathematical module for the classification of cancerous patterns. Nevertheless, none could accurately classify all cancers. In the presented research, a novel method was used for graduating diagnostic power and increasing classification accuracy in classification of thermal images. One reason for using neural networks is that they can simulate a non-linear function and permit development. For assessing the effects of every independent variable on the dependent ones,

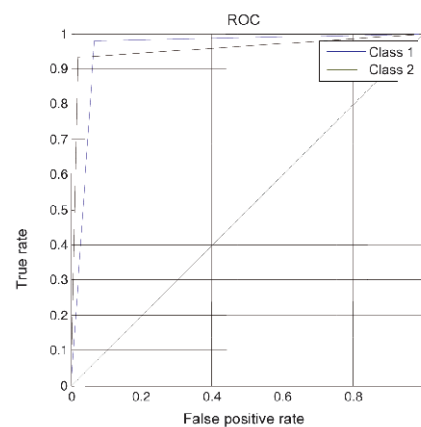


Figure 10. ROC curve of the fuzzy neural network model.

the NN is combined with a genetic algorithm. The optimal result could be able to reduce error by fuzzy logic.

References

1. Usuki H, Onoda Y, Kawasaki S, Misumi T, Murakami M, Komatsubara S, et al. Relationship between thermographic observations of breast tumors and the DNA indices obtained by flow cytometry. *Biomedical Thermology* 1999; 10(4):282-5.
2. West D, Mangiameli P, Ramp R, West V. Ensemble strategies for a medical diagnosis decision support system: A breast cancer diagnosis application. *Eur J Oper Res* 2005; 162:532-51.
3. Sherring and Varsha, 2009. Mediating breast cancer in India. NCA 94th annual convention, San Diego, CA.
4. Sherman DW, Haber J, Noll Hoskins C, Budin WC, Maislin G, Shukla S, et al. The effects of psycho education and telephone counseling on the adjustment of women with early-stage breast cancer. *Appl Nurs Res* 2012; 25(1):3-16.
5. Ng EYK, Sudarshan NM. Numerical computation as a tool to aid thermographic Interpretation. *J Med Eng Technol* 2001; 25:53-60.
6. Baider L, Andritsch E, Goldzweig G, Uziely B, Ever-Hadani P, Hofman G, et al. Changes in psychological distress of women with breast cancer in long-term remission and their husbands. *Psychosomatics* 2004;45(1):58-68.
7. National Cancer Institute: SEER Stat Fact Sheets: Breasts. Available from: <http://www.seer.cancer.gov/statfacts/html/breast.html>.
8. Araujo M.C. Use of the infrared camera to evaluate different diseases in tropical climates and using it together with a database system so as to detect breast cancer. Master's Thesis, Federal University of Pernambuco, Brazil, 2009.
9. Tang J, Rangayyan R, Yang Y, Naqa IE, Xu J. Computer aided breast cancer detection and diagnosis using mammography recent advance. *IEEE Trans Inf Technol Biomed* 2009; 13:236-51.
10. Muralidhar G.S, Bovik A.C, Sampat M.P, Whitman G.J, Haygood T.M, Markey M. Computer-aided diagnosis in breast magnetic resonance imaging. *Mt Sinai J Med* 2011;78: 280-90.
11. Joro R, aperi A.L, arvenp R.J, uukasjarvi T.K, Toivonen T, Saaristo R, Soimakallio S. A dynamic infrared imaging-based diagnostic process for breast cancer. *Acta Radiological* 2009 50(8):860-9.
12. YK Ng E, Kee E.C, Acharya R.U. Advanced technique in breast thermography analysis, in: Proceedings of the 27th Annual Conference on IEEE Engineering in Medicine and Biology, 2005; 710-3.
13. Koay J, Herry C, Frize M. Analysis of breast thermography with an artificial neural network, in: Proceedings of the 26th Annual International Conference on IEEE EMBS, 2004; 1159-62.
14. Kapoor P, Prasad S.V.A.V. Image processing for early diagnosis of breast cancer using infrared images. Institute of Electrical and Electronics Engineers, 2010;3:564-6.
15. Parisky Y.R, Sardi A, Hamm R, Hughes K, Esserman L, Rust S, et al. Efficacy of computerized infrared imaging analysis to evaluate mammographic ally suspicious lesions. *AJR Am J Roentgenol* 2003;180:263-9.
16. Wang J, Chang K.J, Chen C.Y, Chien K.L, Tsai Y.S, Wu Y.M, et al. Evaluation of the diagnostic performance of infrared imaging of the breast: a preliminary study. *Biomedical Engineering Online* 2010;9(3):1-10.
17. Kennedy D, Lee T, Seely D. A comparative review of thermography as a breast screening technique. *Integrative Cancer Therapies* 2009;8: 9-16.
18. Ng E.Y.K. A review of thermography as promising non-invasive detection modality for breast tumor. *International Journal of Thermal Sciences* 2009; 48:849-59.
19. Amalu W.C, Hobbins W.B, Head J.F, Elliot R.L. Infrared imaging of the breast an overview, in: J.D. Bronzino (Ed.), *Biomedical Engineering Handbook*, third ed., Medical Devices and Systems, CRC Press, 2006.
20. Deng Z.S, Liu J. Enhancement of thermal diagnostics on tumors underneath the skin by induced evaporation, in: Proc. 27th Annual Conference of IEEE Engineering in Medicine and Biology, Sanghai, China, 2005.
21. Jennifer M . The effect of abundant precipitation on coal fire subsidence and its implications in Centralia, PA. *International Journal of Coal Geology*, Available online 2012; 17.
22. Qi H and Kuruganti P.T. Detecting breast cancer from thermal infrared images by asymmetry analysis: DTIC Document, 2003.
23. Umadevi V, Raghavan S.V, Jaipurkar S. Interpreter for breast thermogram characterization. *Biomedical Engineering and Sciences (IECBES)*, IEEE EMBS Conference on: IEEE: 2010; 150-4.
24. Keyserlignk, Ahlgren, et al. Infrared imaging of the breast; initial reappraisal using high resolution digital technology in 100 successive cases of stage 1 and 2 breast cancer. *Breast J* 1998;4(4):245-51.
25. Tan TZ, Quek C, Ng GS, Ng EYK. A novel cognitive interpretation of breast cancer thermography with complementary learning fuzzy neural memory structure. *Expert Systems with Applications* 2007;33: 652-66.
26. Ghayoumi Zadeh H, Abaspur Kazerouni I, Haddadnia J. Diagnosis of breast cancer and clustering technique using thermal indicators exposed by infrared images. *Journal of American Science*, 2011; 7(6):281-8.
27. Ghayoumi Zadeh H, Abaspur Kazerouni I, Haddadnia J. Distinguishing breast cancer based on thermal

- features in infrared images. *Canadian Journal on Image Processing and Computer Vision* 2011; 2(6):54-8.
28. Srivastava MS. A measure of skewness and kurtosis and a graphical method for assessing multivariate normality. *Statistics & Probability Letters* 1984; 2(5): 263-7.
 29. Viviani R, Beschoner P, Ehrhard K, Schmitz B, Thöne J. Non-normality and transformations of random fields, with an application to voxel-based morphometry. *Neuro Image* 2007; 35(1): 121-30.
 30. Karimi H, Yousefi F. Application of artificial neural network–genetic algorithm (ANN–GA) to correlation of density in nanofluids. *Fluid Phase Equilibria* 2012; 336(25): 79-83.
 31. Tan TZ, Quek C, Ng GS. Clinical Diagnosis Using Proteomics and Complementary Learning. *Neural Networks, 2006 IJCNN'06 International Joint Conference on; 2006; 2865-72.*
 32. Meng Y. A swarm intelligence based algorithm for proteomic pattern detection of ovarian cancer. *Computational Intelligence and Bioinformatics and Computational Biology, CIBCB'06 IEEE Symposium on: IEEE 2006; 1-7.*
 33. Dhar V, Chou D. Comparison of nonlinear methods for predicting earnings surprises and returns. *IEEE Transactions on Neural Networks* 2001; 12(4): 907-21.
 34. Jang J R, Sun C. Neuro Fuzzy Modelling and Control, *Proc. of the IEEE, 1995; 378-405.*
 35. Kuo RJ, Chen CH, Hwang YC. An intelligent stock trading decision support system through integration of genetic algorithm based on fuzzy neural network and artificial neural network. *Fuzzy Sets and Systems* 2001; 118(1):21-45.
 36. Jang JSR. ANFIS: Adaptive – network - based fuzzy inference system. *IEEE Transactions on Systems, Man, and Cybernetics* 1993; 23(3): 665-85.
 37. Buyukbingol E, Sisman A, Akyildiz M, Alparslan FN, Adejare A. Adaptive neuro fuzzy inference system (ANFIS): A new approach to predictive modeling in QSAR applications: A study of neuro-fuzzy modeling of PCP-based NMDA receptor antagonists. *Bioorganic & Medicinal Chemistry* 2007; 15(12): 4265-82.
 38. Amiryousefi MR, Mohebbia M, Khodaiyan F, Asadi Sh. An empowered adaptive neuro-fuzzy inference system using self-organizing map clustering to predict mass transfer kinetics in deep-fat frying of ostrich meat plates. *Computers and Electronics in Agriculture* 2011;76:89-95.